

## Conditions for the use of infrared camera diagnostics in energy auditing of the objects exposed to open air space at isothermal sky

TADEUSZ KRUCZEK<sup>1</sup>

Silesian University of Technology, Institute of Thermal Technology  
Konarskiego 22, 44-100 Gliwice, Poland

**Abstract** Convective and radiation heat transfer take place between various objects placed in open air space and their surroundings. These phenomena bring about heat losses from pipelines, building walls, roofs and other objects. One of the main tasks in energy auditing is the reduction of excessive heat losses. In the case of a low sky temperature, the radiation heat exchange is very intensive and the temperature of the top part of the horizontal pipelines or walls is lower than the temperature of their bottom parts. Quite often this temperature is also lower than the temperature of the surrounding atmospheric air. In the case of overhead heat pipelines placed in open air space, it is the ground and sky that constitute the surroundings. The aforementioned elements of surroundings usually have different values of temperature. Thus, these circumstances bring about difficulties during infrared inspections because only one ambient temperature which represents radiation of all surrounding elements must be known during the thermovision measurements. This work is aimed at the development of a method for determination of an equivalent ambient temperature representing the thermal radiation of the surrounding elements of the object under consideration placed in open air space, which could be applied at a fairly uniform temperature of the sky during the thermovision measurements as well as for the calculation of radiative heat losses.

**Keywords:** Thermovision diagnostics; Infrared camera; Radiative ambient temperature; Open air space

---

<sup>1</sup>E-mail: tadeusz.kruczek@polsl.pl

## Nomenclature

$\dot{e}_\lambda(\lambda, T)$	– spectral density of black body self-emission for temperature $T$ , resulting from Planck's law, $W/(\mu m m^2)$
$\dot{e}$	– emissive power of black body in spectral range $\lambda' - \lambda''$ at a given temperature $T$ , $W/m^2$
$F$	– surface area, $m^2$
$\dot{h}$	– unit radiosity of surface, $W/m^2$
$r$	– reflectivity of surface
$T$	– temperature, K

## Greek symbols

$\alpha$	– tilt angle between zenith and normal direction of considered surface, °
$\varepsilon$	– emissivity of surface
$\theta$	– zenith angle, ° or rad
$\lambda$	– wave length of thermal radiation, $\mu m$
$\lambda', \lambda''$	– spectral limits of infrared camera, $\mu m$
$\varphi$	– configuration factor

## Subscripts

$d$	– differential or local
$e$	– equivalent or substituting quantity
$G$	– ground
$i, j$	– $i$ th or $j$ th surface or element
$p$	– pyrgeometer
$S$	– sky

## 1 Introduction

Energy auditing of various objects (pipelines, buildings, etc.) is intended to evaluate the possibility of improving energy efficiency of the installations under consideration [1]. The infrared camera measurement results allow to determine the temperature distributions on outer surfaces of examined objects and to calculate the heat losses. The method based on the concept of one-off thermovision measurement of the considered object can be applied [2] to determine the annual heat losses. Knowledge of the heat losses from the analysed objects is of crucial importance in the elaboration of methods for improving the technical conditions and ways of operation of these objects (overhead pipelines, buildings and others) in terms of energy or exergy efficiency [3–7]. The general recommendations are usually gathered in different official documents, standards and other elaborations [1,8] which are a basic tool for engineers dealing with such problems. Obviously, depending on situation, these recommendations can be adjusted properly as the need arises.

In the infrared thermography technique the result of the temperature measurement is influenced by emissivity of the examined surface and the temperature of the surrounding elements [9–13]. The non-contact methods are based on the measurement of radiative heat flux coming from the surfaces taken into consideration. In the situations when the emissivity of the investigated object is less than 100%, the total radiative heat flux from the tested surface consists of two parts. The first part presents the self-emission heat flux whereas the second part is the radiation flux which comes from surroundings and is reflected by the considered surface. The problem arises when the ambient temperature for objects in open air space needs to be determined. Generally, the surroundings of the objects which are placed in open air space consist of two elements, namely the hypothetical sky surface and the ground surface. Normally, the temperature of these elements is different and the ambient temperature value which should be entered into the measuring system of the infrared (IR) camera is not known. To solve this problem, an innovative method for the determination of the equivalent ambient temperature in the case of nonisothermal surroundings has been proposed in this work. This technology consists in the conversion of two-element and nonisothermal surroundings into one-element isothermal surroundings where a method of radiosity and configuration factors has been applied. The surroundings containing two isothermal elements (sky and ground) were considered in further analysis. The next problem is the determination of sky temperature responsible for thermal radiation. In order to determine this temperature the measurement with the use of a long wave (LW) infrared camera with a special configuration of its measurement parameters has been proposed [14]. In this measurement technology the sky is treated as a hemispherical shell. In the case of not cloudy weather the sky temperature is relatively low and diversified whereas during cloudy nights this temperature is relatively high and quite uniform [15]. Such method of determination of sky thermal radiation with the use of infrared camera measurement has been successfully verified [14]. To verify the developed method, the results obtained with the use of a LW IR camera and measurement results obtained by means of the pyrgeometer have been compared. The results of this comparison are quite satisfactory.

During the measurements the following measuring devices were applied: an infrared camera ThermaCAM SC2000 FLIR and pyrgeometer CGR4 Kipp&Zonen.

## 2 Influence of the surrounding temperature on the results of infrared temperature measurement

### 2.1 Radiative geometric configuration factors

The configuration factors, expressing thermodynamic interactions of the surface with its surrounding environment, play an important role in the mathematical description of radiative heat transfer. Elementary (differential) configuration factor  $\varphi_{d1-d2}$  deals with a relation between two differential area elements  $\mathbf{d}F_1$  and  $\mathbf{d}F_2$ , [16,17], and it is defined by means of the relation  $\varphi_{d1-d2} = (\cos \beta_1 \cos \beta_2 / (\pi a^2)) \mathbf{d}F_2$ , where  $\beta_1, \beta_2$  – denote angles between the line connecting differential area elements  $\mathbf{d}F_1, \mathbf{d}F_2$  and normal directions to these elements, respectively,  $a$  – is the distance between aforementioned area elements. For differential area element  $\mathbf{d}F_1$  and finite area  $F_2$ , the so-called local configuration factor  $\varphi_{d1-2}$  is defined [16,17]. This factor is obtained by a single integration of factor  $\varphi_{d1-d2}$  over  $F_2$  what can be written as  $\varphi_{d1-2} = \int_{F_2} \varphi_{d1-d2} \mathbf{d}F_2$ . These factors are used during the analysis of interactions between the infinitely small area  $\mathbf{d}F_1$  and area  $F_2$  (finite or infinitely large). For finite areas  $F_1$  and  $F_2$  the expression  $\varphi_{d1-2}$  should be integrated once again over  $F_1$ . Then, to obtain an average value of the configuration factor (CF) for the area  $F_1$ , the obtained result should be divided by  $F_1$ . As a result, the average configuration factor  $\varphi_{1-2}$  is obtained  $\varphi_{1-2} = (1/F_1) \int_{F_1} \varphi_{d1-2} \mathbf{d}F_1$ . The average configuration factors (CFs) are applied in the analysis of the total thermal interaction of the whole isothermal surfaces  $F_1$  and  $F_2$ . The described factors are significant for further considerations.

### 2.2 Mechanism of the influence of surrounding elements temperature on infrared temperature measurement

During thermovision observation of tested surface ‘1’ (Fig. 1), the IR camera records a sum of self-emission of the considered object and radiosity flux of surroundings reflected by the surface under consideration. In further considerations of this Section the average CFs will be used. This is justified in case of the analysis of an average ambient influence on the temperature of large finite surfaces. For a small size of the tested surface ‘1’ the local CFs are recommended. The resulting conclusions are valid for both cases. For the simplicity of analysis a potential presence of any gas between the tested object and IR camera is omitted. The aforementioned sum of radia-

tion fluxes is the radiosity of the tested surface. In order to calculate this value for considered surfaces (Fig. 1), the balances of radiosity have been formulated:

$$F_1 \dot{h}_1 = \varepsilon_1 F_1 \dot{e}_1 + r_1 F_2 \dot{h}_2 \varphi_{2-1} , \quad (1)$$

$$F_2 \dot{h}_2 = \varepsilon_2 F_2 \dot{e}_2 + r_2 F_1 \dot{h}_1 \varphi_{1-2} + r_2 F_2 \dot{h}_2 \varphi_{2-2} . \quad (2)$$

Further, the closure principle  $\sum_{j=1}^{j=2} \varphi_{i-j} = 1$  (for  $i = 1$  or  $i = 2$ ) and reciprocity principle  $F_1 \varphi_{1-2} = F_2 \varphi_{2-1}$  are applied. After making obvious assumptions that  $\varepsilon_2 = 1$  (the radiation flux emitted by the considered object is entirely absorbed by the surrounding elements, therefore also  $r_2 = 0$ ) as well as  $\varphi_{1-2} = 1$  (the surface '1' is flat or convex so  $\varphi_{1-1} = 0$ ), after some manipulations an accurate relation expressing the unit flux of radiation energy  $\dot{h}_1$  (its radiosity) coming from surface '1' is obtained

$$\dot{h}_1 = \varepsilon_1 \dot{e}_1 + (1 - \varepsilon_1) \dot{e}_2 \quad \text{or} \quad \dot{h}_1 = \varepsilon_1 \dot{e}_1(T_1) + (1 - \varepsilon_1) \dot{e}_2(T_2) , \quad (3)$$

where  $\dot{e}_1 = \dot{e}_1(T_1)$  and  $\dot{e}_2 = \dot{e}_2(T_2)$ . In this case the calculated quantity is  $\dot{e}_1$  because quantity  $\dot{h}_1$  is known owing to IR camera measurement whereas quantity  $\dot{e}_2$  is calculated on the basis of temperature  $T_2$  entered into the IR camera measurement system.

To represent the influence of ambient conditions on the measurement result by means of only one temperature value, the conversion method of nonisothermal two-element surroundings (Fig. 2) into one-element isothermal surroundings has been proposed which ensures keeping their radiation influence on the considered surface in terms of quantity [9].

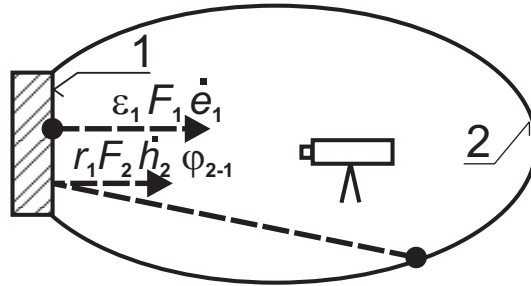


Figure 1: Scheme of heat transfer in the measurement space: 1 – surface of object under investigation, '1', 2 – one-element isothermal surroundings '2'.

For this purpose the method of radiosity balances was applied again [16,17]

$$F_1 \dot{h}_1 = F_1 \varepsilon_1 \dot{e}_1 + r_1 \varphi_{1-1} F_1 \dot{h}_1 + r_1 \varphi_{2-1} F_2 \dot{h}_2 + r_1 \varphi_{3-1} F_3 \dot{h}_3 , \quad (4)$$

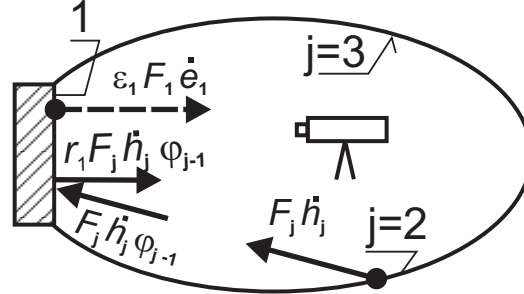


Figure 2: Tested surface '1' surrounded by system of surfaces '2' and '3' treated as isothermal objects.

$$F_2 \dot{h}_2 = r_2 \varphi_{1-2} F_1 \dot{h}_1 + F_2 \varepsilon_2 \dot{e}_2 + r_2 \varphi_{2-2} F_2 \dot{h}_2 + r_2 \varphi_{3-2} F_3 \dot{h}_3, \quad (5)$$

$$F_3 \dot{h}_3 = r_3 \varphi_{1-3} F_1 \dot{h}_1 + r_3 \varphi_{2-3} F_2 \dot{h}_2 + F_3 \varepsilon_3 \dot{e}_3 + r_3 \varphi_{3-3} F_3 \dot{h}_3. \quad (6)$$

The following assumptions were made: reflectivity of the considered surfaces is of diffuse character, the presence of gas in the considered space is omitted, the considered surface is flat or convex ( $\varphi_{1-1} = 0$ ) and all surrounding elements ( $i > 1$ ) meet the conditions  $\varepsilon_i = 1.0$  ( $r_i = 0.0$ ). Moreover, in further transformations of the aforementioned relations the closure and reciprocity principles have been applied [16,17]. Therefore, the equations expressing the radiosities of the considered elements of the measurement system in case of two-element surroundings (Fig. 2) can be written as

$$\dot{h}_1 = \varepsilon_1 \dot{e}_1 + r_1 \varphi_{1-2} \dot{h}_2 + r_1 \varphi_{1-3} \dot{h}_3, \quad (7)$$

$$\dot{h}_2 = \dot{e}_2, \quad (8)$$

$$\dot{h}_3 = \dot{e}_3. \quad (9)$$

Finally, a relationship presenting the unit radiosity of the considered surface in case of nonisothermal surroundings consisting of two surfaces closing the considered space takes the following form:

$$\dot{h}_1 = \varepsilon_1 \dot{e}_1 + r_1 \varphi_{1-2} \dot{e}_2 + r_1 \varphi_{1-3} \dot{e}_3 = \varepsilon_1 \dot{e}_1 + (1 - \varepsilon_1)(\varphi_{1-2} \dot{e}_2 + \varphi_{1-3} \dot{e}_3). \quad (10)$$

After the comparison of above equation with a similar one for one-element surroundings which is applied in the IR camera measurement system (Eq. (3)), the following is obtained:

$$\dot{h}_1 = \dot{e}_1 \varepsilon_1 + \dot{e}_e r_1 = \dot{e}_1 \varepsilon_1 + \dot{e}_e (1 - \varepsilon_1). \quad (11)$$

To keep the equivalence of nonisothermal two-element surroundings and the isothermal ones, the radiosity of the tested surfaces for both cases must be identical. After comparison of right-hand sides of Eqs. (10) and (11), a relationship which provides a basis for the calculation of the equivalent temperature of substituting isothermal surroundings is obtained:

$$\dot{e}_e = \dot{e}_e(T_e) = \varphi_{1-2}\dot{e}_2 + \varphi_{1-3}\dot{e}_3 \quad (12)$$

or

$$\dot{e}_e = \int_{\lambda'}^{\lambda''} \dot{e}_\lambda(\lambda, T_e) \mathbf{d}\lambda = \varphi_{1-2} \int_{\lambda'}^{\lambda''} \dot{e}_\lambda(\lambda, T_2) \mathbf{d}\lambda + \varphi_{1-3} \int_{\lambda'}^{\lambda''} \dot{e}_\lambda(\lambda, T_3) \mathbf{d}\lambda, \quad (13)$$

where  $\dot{e}_\lambda$  denotes spectral density of black body self-emission resulting from Planck's law (see nomenclature). The Eq. (13) has the general shape and enables determination of the equivalent ambient temperature,  $T_e$ , of the tested object in the case of nonisothermal surroundings. The equivalent temperature  $T_e$  is defined by the second term of Eq. (13) in which it occurs in the implicit form. The value of this temperature can be determined after calculation of a value of the third term of Eq. (13) where values  $T_2$  and  $T_3$  are known.

### 3 Celestial vault as an isothermal element of surroundings of the tested object

#### 3.1 An example of the celestial vault temperature measurement by means of the LW infrared camera

The temperature of sky depends on weather conditions. The conditions suitable for infrared measurements occur at nights with the sky covered by a uniform layer of clouds of stratus or stratocumulus types [15]. In case of a cloudless sky, the sky temperature in the zenith direction is always relatively low whereas in other directions it is much higher. This phenomenon is caused by the increase of the length of the path radiation beam in atmospheric air [18]. In Fig. 3 the example of sky temperature measurement with the use of the LW infrared camera can be seen. It should be remembered that sky temperature measured by the infrared camera has an apparent character because there is no unambiguously defined surface. This temperature results from the infrared radiation of the sky in the spectral range of infrared camera operation.

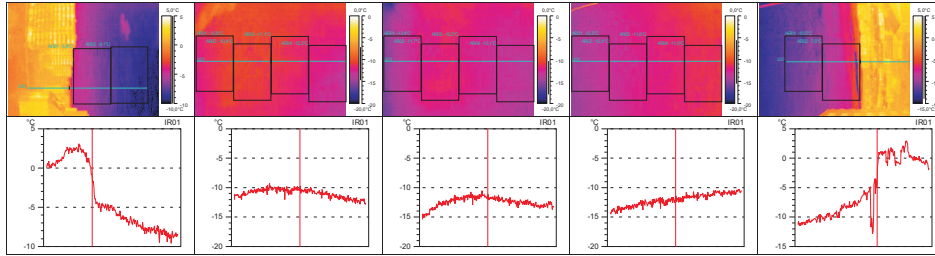


Figure 3: Apparent temperature of the sky measured within the zenithal angle range  $(-90^\circ; +90^\circ)$ .

### 3.2 A geometrical model of sky radiation

During the analysis of radiative heat exchange between objects in open air space and the surrounding elements, various calculation models can be potentially applied. Due to practical reasons, in the case of fairly uniform covering of the sky (S) by clouds, the radiation of atmosphere has been substituted by the radiation of an apparent isothermal horizontal infinitely large plane. Also the ground surface (G) has been approximated by means of a horizontal infinite plane, Fig. 4. Depending on the tilt of the considered surface in relation to zenith direction characterized by angle  $\alpha$ , the values of local configuration factors expressing the interactions of the considered surface  $dF_1$  and elements of the surroundings will be varying. These values can be calculated from the relations [19,20]

$$\varphi_{d1-3} = 0.5(1 + \cos \alpha) , \quad (14)$$

$$\varphi_{d1-2} = 0.5(1 - \cos \alpha) . \quad (15)$$

Figure 5 presents the values of local CF between element  $dF_1$  and the whole part of the sky seen from this elementary area as well as similar CF for  $dF_1$  and the ground. They can be used for thermal calculations in the case when the sky and ground are treated as two separate isothermal elements of the surroundings. The obtained values of CFs make it possible to determine the equivalent temperature ( $T_e$ ) of the surroundings of the considered surface during their thermovision inspection. This temperature can be calculated on the basis of Eq. (13). The aforementioned configuration factors can be also used during the calculation of local radiative heat losses into the environment along the pipeline circumference or other surfaces.



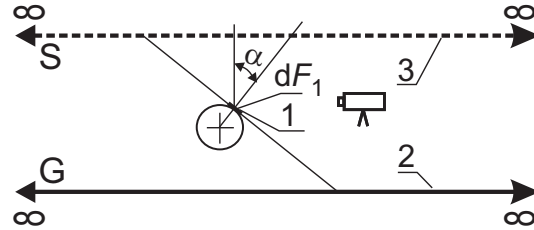


Figure 4: A geometrical model of considered object surroundings consisting of ground ( $G$ ) and sky ( $S$ ).

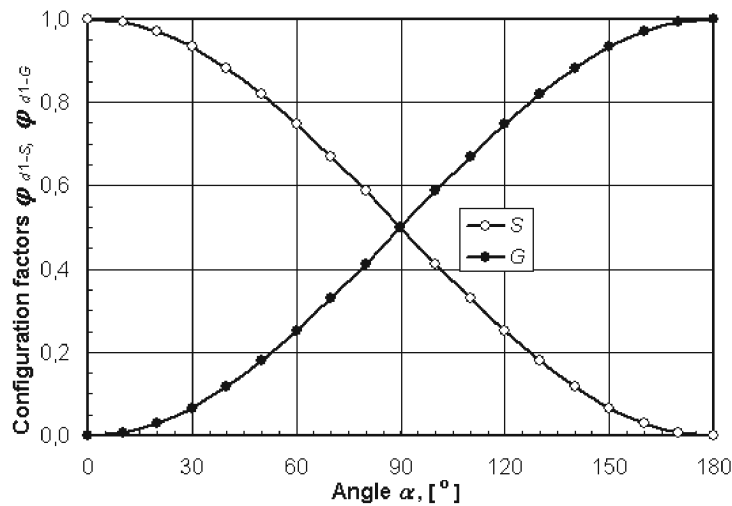


Figure 5: Local CFs between the considered surface element and the whole sky ( $S$ ) or ground ( $G$ ) as a function of the surface tilt angle  $\alpha$ .

#### 4 Example calculation of the equivalent ambient temperature for infrared measurements in open air space

On the basis of Eq. (13) and the obtained values of CFs (Fig. 5), the equivalent radiative ambient temperature can be determined. The data shown in Fig. 5 are suitable for calculation of the aforementioned equivalent ambient temperature only in case of isothermal sky because they present the interactions between the chosen points and the whole celestial vault or ground. The ground can usually be treated as the isothermal surface with a good approximation. The results of calculations are presented in Fig. 6. It

should be emphasized that these results are valid for the LW infrared camera with its typical operation spectral range, i.e. 7.5–13  $\mu\text{m}$ . The presented concept of the use of local CFs can be also applied for the calculation of local heat losses into the environment from the considered surfaces. However, in this case the full spectral range ( $0 \div +\infty$ ) should be taken into account during the calculation of the equivalent ambient temperature.

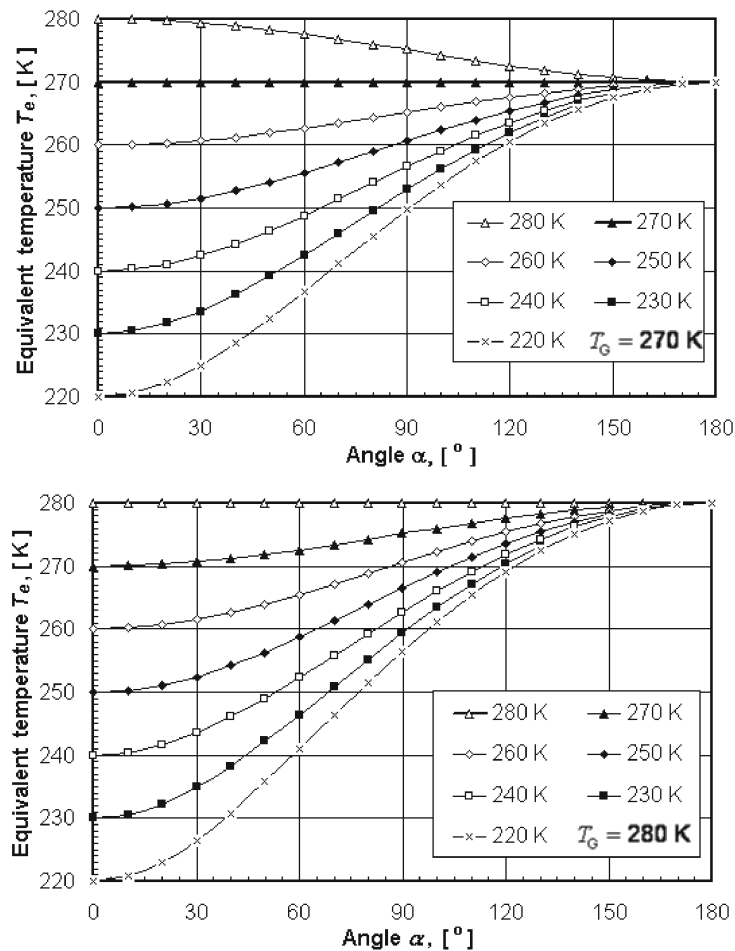


Figure 6: Equivalent temperature of one-element surroundings as a function of the tilt angle  $\alpha$ , for ground temperature  $T_G$  and apparent sky temperature specified in the diagram legend.

## 5 Measurement of the temperature of sky and its thermal radiation by means of a long wave infrared camera

In this work it has been proposed to measure the apparent temperature of the sky by means of a LW infrared camera, Figs. 3, 7, and 8. The temperature value indicated by the IR camera is not a temperature of the atmosphere but the result reflects the thermal radiation of the atmosphere within the spectral range of the LW IR camera operation, i.e., 7.5–13  $\mu\text{m}$ . This spectral range is coincident with the so-called atmospheric window where the thermal radiation of the atmosphere is relatively low. However, this measured temperature can be used for the calculation of thermal radiation flux emitted by the atmosphere within aforementioned spectral range. The numerical calculations realized with the use of the spectral line model of gases radiation HITEMP [21,22] showed that for atmospheric conditions the atmosphere can be treated as black body within the spectral ranges of its radiative bands [14]. Therefore, the total thermal radiation flux of the atmospheric air from any direction can be determined as the sum of emissions within the so-called windows (spectral ranges of low radiation of the atmosphere) and active bands

$$\dot{e} = \sum_{i=1}^n \int_{\lambda_{p,i}}^{\lambda_{k,i}} \dot{e}_{\lambda}(\lambda, T_{cm}) \mathbf{d}\lambda + \sum_{l=1}^m \int_{\lambda_{p,l}}^{\lambda_{k,l}} \dot{e}_{\lambda}(\lambda, T_{at}) \mathbf{d}\lambda, \quad (16)$$

where:  $\lambda_{p,i}$ ,  $\lambda_{k,i}$  and  $\lambda_{p,l}$ ,  $\lambda_{k,l}$  – spectral limits of ranges for  $i$ th window and  $l$ th active radiation band of atmospheric air,  $n$ ,  $m$  – numbers of atmospheric windows and active bands taken into consideration within operation spectral range of pyrgeometer ( $n = 2$ ,  $m = 2$ ), respectively,  $T_{at}$  – temperature of atmospheric air,  $T_{cm}$  – temperature measured by the LW IR camera. Next, for each  $j$ th assumed spherical band of celestial vault with its temperature  $T_j$  (Fig. 8), radiation flux  $\dot{e}_j$  emitted by this band was calculated on the basis of relation (16). Finally, the total energy flux  $\dot{e}_S$  irradiating the unit horizontal surface can be calculated from relation

$$\dot{e}_S = \sum_{j=1}^N \dot{e}_j \varphi_{p-j}, \quad (17)$$

where:  $N$  – number of spherical bands,  $\varphi_{p-j}$  – CF between horizontal surface of pyrgeometer detector and  $j$ th spherical band.

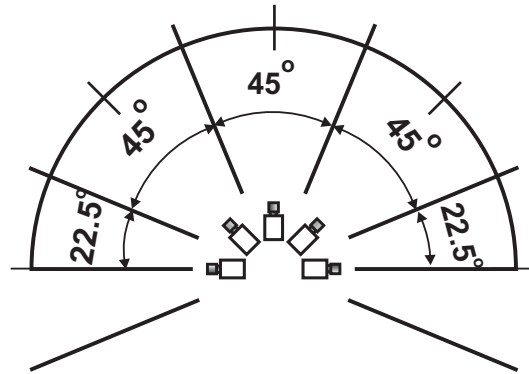


Figure 7: Scheme of sky temperature measurement by means of the LW IR camera.

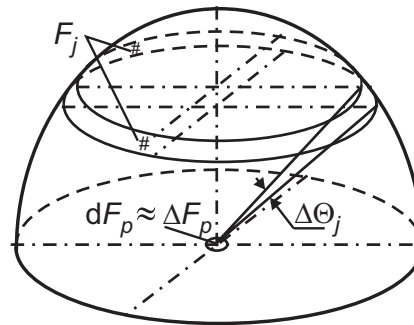


Figure 8: Geometrical presentation of heat transfer model for the measurement of sky thermal radiation by means of the IR camera and the pyrgeometer.

The energy flux was calculated from relation (17) and simultaneously for the same moment was measured by pyrgeometer with a spectral range of operation  $4.5\text{--}42\ \mu\text{m}$ . The results of comparison analysis are presented in Figs. 9 and 10. They are quite satisfactory although there are some discrepancies in the obtained results which are of about 5–8%, Fig. 10. A few circumstances can be mentioned as the reasons for these discrepancies. The first is a method of sky scanning which was performed only once along a vertical plane. The second reason, the more important one, is the temperature increase in the upper parts of the atmosphere due to condensation of water vapour contained in the atmospheric air. It is not possible to estimate in a simple way the scale of this phenomenon in terms of quantity. In order to do it, the use of more advanced methods is necessary, which constitutes another extended research problem exceeding the scope of this work [23,24].

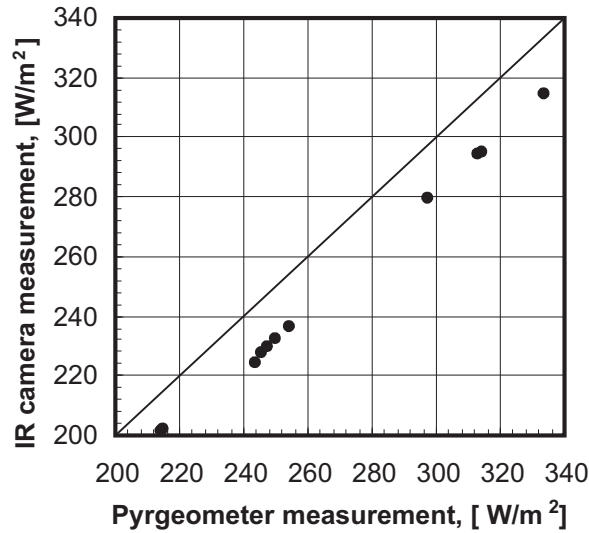


Figure 9: Comparison of specific infrared emission of the sky measured by means of the pyrometer with emission calculated on the basis of the sky temperature measurement with the use of the LW IR camera.

This concept can also be applied during the calculations of the local radiative heat losses from the surface placed in open air space at isothermal sky and tilted at angle  $\alpha$ . For this purpose a substituting radiative ambient temperature  $T_{am}$  calculated as follows can be applied:

$$T_{am} = \sqrt[4]{\dot{e}_{\alpha}/(5.67 \times 10^{-8})} \quad \text{and} \quad \dot{e}_{\alpha} = \dot{e}_S \varphi_{d1-S} + \dot{e}_G \varphi_{d1-G}, \quad (18)$$

where  $S, G$  deals with sky and ground seen from the considered surface, respectively.

In [8] there is an following recommendation for calculation of radiative heat losses from the considered object ('obj'):

$$\dot{q}_{loss} = 5.67 \times 10^{-8} \varepsilon_{obj} (T_{obj}^4 - T_{am}^4) \quad (19)$$

but unfortunately the way of determining the ambient temperature has not been explained.

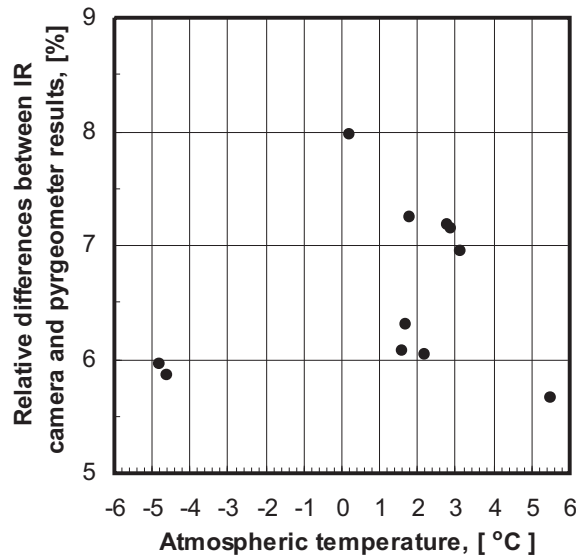


Figure 10: Comparison of relative differences between sky emission measured by means of the pygeometer and emission calculated on the basis of the sky temperature measurement with the use of the LW IR camera.

## 6 Final remarks

The work deals with the infrared diagnostics of the objects in open air space and contains descriptions of all elements of measurement procedure. The paper is particularly innovative owing to the developed method of the ambient radiation temperature determination (called the equivalent ambient temperature) for thermovision measurements with nonisothermal elements of surroundings. The proposed method allows the thermographers to determine a proper value of substitute temperature representing all elements surrounding and closing the space around the tested surface, i.e. equivalent ambient temperature. This temperature sometimes is also called 'the reflected temperature'. The value of the ambient temperature must be entered into the IR camera during the measurements.

During the IR camera measurements in open air space, the sky is one of the surrounding elements. Therefore, to apply the mentioned above method, the temperature of the sky should be known. For this purpose, the use of the LW IR camera has been proposed. The sky temperature directly measured by the camera should be used in the calculations of the equivalent

ambient temperature which is necessary during the IR camera measurement of the temperature of the object under consideration.

For the calculation of radiative heat losses the temperature representing the thermal radiation of the atmosphere within the whole spectral range must be known. Hence, the method of determining total radiation of the sky with the use of IR camera measurement of the sky temperature has been developed. This method has been positively verified by comparison with measurement results obtained from the pyrgeometer. Afterwards, the substituting radiative ambient temperature can be calculated. This temperature is suitable for the calculation of local radiation heat losses according to general recommendations included in the European standard [8].

**Acknowledgements** The scientific work was supported by Faculty of Energy and Environmental Engineering of the Silesian University of Technology within the statutory research.

*Received 10 December 2014*

## References

- [1] GÓRZYŃSKI J.: *Energy auditing*. National Agency of Energy Conservation (NAPE), Warsaw 2000 (in Polish).
- [2] KRUCZEK T.: *Determination of annual heat losses from heat and steam pipeline networks and economic analysis of their thermomodernisation*. *Energy* **62**(2013), 120–131.
- [3] DALLA ROSA A., LI H., SVENDSEN S.: *Method for optimal design of pipes for low-energy district heating, with focus on heat losses*. *Energy* **36**(2011), 5, 2407–2418.
- [4] LI HONGWEI, SVENDSEN S.: *Energy and exergy analysis of low temperature district heating network*. *Energy* **45**(2012), 1, 237–246.
- [5] BIAŁECKI R., KRUCZEK T.: *Frictional, diathermal flow of steam in a pipeline*. *Chem. Eng. Sci.* **51**(1996), 19, 4369–4378.
- [6] FURMAŃSKI P., WIŚNIEWSKI T.: *Influence of radiation scattering on heat transfer and determination of properties of thermal insulations*. *Thermal Cond.* **26**(2004), 400–411.
- [7] SEKRET R., NITKIEWICZ A.: *Exergy analysis of the performance of low-temperature district heating system with geothermal heat pump*. *Arch. Thermodyn.* **35**(2014), 1, 77–86.
- [8] PN-EN ISO 12241 *Thermal insulation for building equipment and industrial installations – Calculation rules*, 2001.

- [9] KRUCZEK T.: *Analysis of the influence of external conditions on thermovision measurement results*. In: Proc. 5th Conf. *Thermography and Thermometry in Infrared TTP 2002*, Ustroń, 2002, 327–332 (in Polish).
- [10] KLIMPEL A., KRUCZEK T., LISIECKI A., JANICKI D.: *Experimental analysis of heat conditions of the laser braze welding process of copper foil absorber tube for solar collector elements*. *Weld. Int.* **27**(2013), 6, 434–440.
- [11] KLIMPEL A., LISIECKI A., SZYMAŃSKI A., HOULT A.: *Numerical and experimental determination of weld pool shape during high-power diode laser welding*. In: Proc. SPIE 5229(2003), 247–250, Laser Technology VII, Applications of Lasers, 6 Oct. 2003.
- [12] ORZECZOWSKI T.: *Determining local values of the heat transfer coefficient on a fin surface*. *Exp. Therm. Fluid Sci.* **31**(2007), 8, 947–55.
- [13] NEMEC P., ČAJA A., LENHARD R.: *Visualization of heat transport in heat pipes using thermocamera*. *Arch. Thermodyn.* **31**(2010), 4, 125–132.
- [14] KRUCZEK T.: *Use of LW infrared camera for measurement of sky thermal radiation*. *MAaM* **59**(2013), 9, 905–908 (in Polish).
- [15] DULSKI R., SOSNOWSKI T., POLAKOWSKI H.: *A method for modelling IR images of sky and clouds*. *Infrared Phys. Techn.* **54**(2011), 53–60.
- [16] HOWELL J.R., SIEGEL R., MENGÜÇ M.P.: *Thermal Radiation Heat Transfer*. CRC Press Taylor&Francis Group, New York 2011.
- [17] JESCHAR R., KOSTOWSKI E., ALT R.: *Thermal radiation*. Internat. Studies in Science and Engineering, Tech. Universität Clausthal, Silesian Univ. of Technology, Gliwice 2004 (in German).
- [18] AWANOU C.N.: *Clear sky emissivity as a function of the zenith direction*. *Renew. Energ.* **13**(1998), 2, 227–248.
- [19] HOWELL J.R.: *A catalog of radiation heat transfer configuration factors*, 3rd Edn., 2010, <http://www.thermalradiation.net/indexCat.html>.
- [20] RUDNICKI Z.: *Mathematical Modelling of Radiative Heat Transfer*. Wyd. Politechniki Śląskiej, Gliwice 2003 (in Polish).
- [21] ROTHMAN L.S., GORDON I.E., BARBER R.J. ET AL.: *HITEMP, the high-temperature molecular spectroscopic database*. *J. Quant. Spectrosc. Ra.* **111**(2010), 15, 2139–2150.
- [22] WĘCEL G., OSTROWSKI Z., KOZOLUB P.: *Absorption line black body distribution function evaluated with proper orthogonal decomposition for mixture of CO<sub>2</sub> and H<sub>2</sub>O*. *Int. J. Numer. Method. H.* **24**(2014), 4, 932–948.
- [23] BERGER X., BATHIEBO J., KIENO F., AWANOU C.N.: *Clear sky radiation as a function of altitude*. *Renew. Energ.* **2**(1992), 2, 139–157.
- [24] CHEN X., WEI H., YANG P., JIN Z., BAUM B.A.: *An efficient method for computing atmospheric radiances in clear-sky and cloudy conditions*. *J Quant. Spectrosc. Ra.* **112**(2011), 109–118.